

Noise enhanced phase synchronization and coherence resonance in sets of chaotic oscillators with weak global coupling

István Z. Kiss, Yumei Zhai, and John L. Hudson

Department of Chemical Engineering, 102 Engineers' Way, University of Virginia, Charlottesville, Virginia 22904-4741

Changsong Zhou and Jürgen Kurths

Institute of Physics, University of Potsdam PF 601553, 14415 Potsdam, Germany

(Received 23 May 2002; accepted 19 August 2002; published 21 February 2003)

The effect of noise on phase synchronization in small sets and larger populations of weakly coupled chaotic oscillators is explored. Both independent and correlated noise are found to enhance phase synchronization of two coupled chaotic oscillators below the synchronization threshold; this is in contrast to the behavior of two coupled periodic oscillators. This constructive effect of noise results from the interplay between noise and the locking features of unstable periodic orbits. We show that in a population of nonidentical chaotic oscillators, correlated noise enhances synchronization in the weak coupling region. The interplay between noise and weak coupling induces a collective motion in which the coherence is maximal at an optimal noise intensity. Both the noise-enhanced phase synchronization and the coherence resonance numerically observed in coupled chaotic Rössler oscillators are verified experimentally with an array of chaotic electrochemical oscillators. © 2003 American Institute of Physics. [DOI: 10.1063/1.1513081]

The subject of this paper is the interplay of two phenomena of importance in nonlinear dynamics: synchronization and noise-induced effects. In classical studies of sets of periodic oscillators with a frequency distribution, the addition of weak global coupling can lead to a transition to synchronization in which many of the elements obtain the same frequency and the phases become locked; the addition of noise has a degrading effect on the synchronous motion. A phase variable may also be defined in chaotic systems. Weak coupling can then produce phase synchronization in which the phases are locked although the amplitudes are uncorrelated. Noise can degrade the phase synchronization as it does in the periodic systems: noise induces phase slips of locked oscillators. On the other hand, noise can play a constructive role in enhancing the synchronization of chaotic systems. Two uncoupled identical chaotic systems can achieve complete synchronization under the influence of a common noise. Noise can also produce amplification of a weak signal (stochastic resonance) or induce coherent oscillations in excitable and damped oscillatory systems (coherence resonance). In this paper we explore the effects of noise on phase synchronization with numerical simulations on small sets and larger populations of coupled nonidentical chaotic Rössler oscillators. Both noise induced phase synchronization and coherent mean field oscillations are seen in large populations. These effects are confirmed in laboratory experiments with arrays of chaotic electrochemical oscillators.

is of significance in biology^{3–7} and engineering (e.g., communications,⁸ high power lasers,⁹ and microwave systems¹⁰). In coupled periodic oscillators, the systems adjust their time scales to achieve locking of frequencies and phases due to weak interaction.^{1,2,11} The notation of synchronization has been extended to include a variety of phenomena in the context of interacting chaotic systems, such as complete synchronization (CS) (Refs. 12–14) and phase synchronization (PS).^{15,16} PS is a weak form of synchronization in which there is a bounded phase difference of two signals. PS occurs at a much weaker coupling strength than CS; in the latter both the phases and amplitudes are identical.

Noise and heterogeneity are unavoidable in experimental and natural systems. Therefore, it is of interest to explore the effects of noise on the robustness of the synchronization process. Noise influences synchronization in different ways. In CS of coupled chaotic systems noise may amplify the synchronization error to generate intermittent loss of synchronization.^{17–20} On the other hand, identical systems which are not coupled but subjected to a common noise may achieve CS at a large noise intensity; this has been demonstrated both in periodic^{21,22} and chaotic^{23–27} systems. Internal noise induced bursts in non-coupled sensories may achieve stochastic PS under a common external noise.²⁸ In PS of coupled phase locked periodic²⁹ and chaotic³⁰ oscillators noise can induce phase slips, i.e., it has a degrading effect.

The constructive role of noise has been studied extensively in the context of stochastic resonance (SR) (Refs. 31–34) and coherence resonance (CR).^{35–37} With SR, noise can optimize the response of a nonlinear system to a weak external signal. SR has also been studied from the viewpoint of noise-enhanced phase synchronization of the switching events to the external signal, because noise controls the average switching rate of the system and the response is opti-

I. INTRODUCTION

The study of coupled oscillators is of importance in many disciplines of science.^{1,2} Synchronization of oscillators

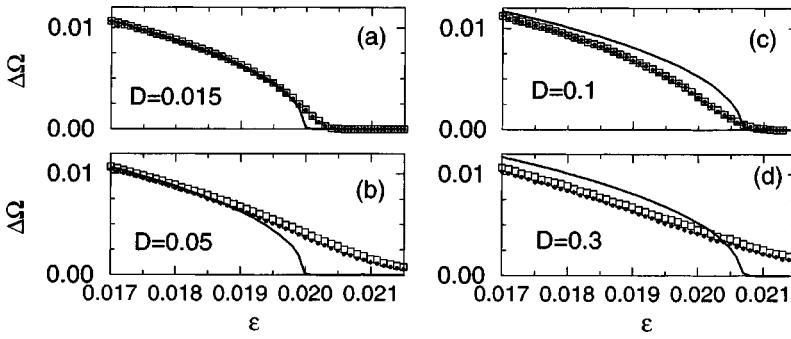


FIG. 1. Frequency difference $\Delta\Omega$ versus coupling strength ϵ . Solid lines: noise-free case $D=0$; open squares: independent noise $R=0$; filled circles: common noise $R=1$. Left panel: two coupled van der Pol periodic oscillators; right panel: two coupled chaotic Rössler oscillators. Both have $\Delta\omega=0.02$.

mal when it is close to that of the external signal.^{34,38–40} By CR, noise alone can produce coherent behavior in dynamical systems. CR has been studied mainly in excitable systems^{35–37} and recently, in systems with coexisting attractors.^{41,42} In distributed (sub)excitable media spatially independent noise can induce traveling waves⁴³ and global oscillations.⁴⁴ Noise induced coherence can be significantly enhanced when the elements are coupled, known as array enhanced CR.^{45–47}

In this paper we study effects of noise on synchronization and coherence of coupled chaotic oscillators with different natural frequencies. Although noise induces phase slips and degrades coherence in the phase locked region, it may significantly enhance PS outside this region. Numerical simulations are carried out with two coupled nonidentical Rössler oscillators and PS of the chaotic systems is analyzed through phase locking of unstable periodic orbits (UPOs). A brief account of results on the two-oscillator system has been published in a recent letter.⁴⁸ In the present contribution, we expand the discussion of phase synchronization of two chaotic oscillators and we extend the studies to populations of chaotic oscillators with both simulations and experiments. The effects of local and global noise on PS and coherent collective behavior of populations of oscillators are studied. The numerical results are confirmed in laboratory experiments using a chemical system; the electrodisolution of an array of nickel electrodes in sulfuric acid solution is studied under chaotic conditions. The same system has been used to explore phase synchronization,⁴⁹ dynamical clustering, and identical synchronization.^{50–52} Here we apply the system as a testbed to verify the effects of noise on weakly coupled populations of chaotic oscillators.

II. NUMERICAL RESULTS

Numerical simulations have been carried out with coupled chaotic Rössler oscillators which display coherent phase dynamics. We consider systems of two coupled and an ensemble of a large number of globally coupled oscillators with different natural frequencies.

To take correlation of noise into account, we consider that the added noise $D\xi_i(t)$ to the i th oscillator is composed of a common part $e(t)$ and an independent part $\eta_i(t)$, satisfying

$$\xi_i(t) = \sqrt{R}e(t) + \sqrt{1-R}\eta_i(t). \quad (1)$$

Both $e(t)$ and $\eta_i(t)$ are assumed to be Gaussian noise, i.e., $\langle e(t)e(t-\tau) \rangle = \delta(\tau)$ and $\langle \eta_i(t)\eta_j(t-\tau) \rangle = \delta_{ij}\delta(\tau)$. A global random forcing is relevant in neuroscience^{53,54} and in ecological systems,⁵⁵ where different populations may be exposed to a similar environmental fluctuations. This description in Eq. (1) allows independent variations of the correlation R between ξ_i and ξ_j and the noise intensity D .

A. Two coupled oscillators

For comparison with chaotic oscillators, we start with two coupled noisy periodic oscillators: the van der Pol oscillators,

$$\ddot{x}_{1,2} - (1 - x_{1,2}^2)\dot{x}_{1,2} + \omega_{1,2}^2 x_{1,2} = \epsilon(\dot{x}_{2,1} - \dot{x}_{1,2}) + D\xi_{1,2}. \quad (2)$$

The natural frequencies are $\omega_1=0.99$ and $\omega_2=0.97$. Introducing phase ϕ and amplitude A as

$$A_i^2 = x_i^2 + y_i^2, \quad \tan \phi_i = y_i/x_i, \quad (3)$$

with $y_i = \dot{x}_i$, PS of the noise-free oscillators is described by the dynamics of the phase difference $\Delta\dot{\phi} = \Delta\omega - \epsilon \sin \Delta\phi$. Perfect phase-locking is achieved for $\epsilon > \epsilon_{ps} = \Delta\omega$, where the system is stable at a local minimum of a tilted periodic potential $U(\Delta\phi) = -\Delta\phi\Delta\omega - \epsilon \cos \Delta\phi$. Noise may kick the system over the energy barrier and induce phase slips. Typical PS behavior of coupled noisy van der Pol oscillators is shown in Figs. 1(a) and 1(b) by the average frequency difference $\Delta\Omega = |\langle \Delta\dot{\phi} \rangle|$. It is seen that both common and independent noise degrade the phase synchronization. This has been previously shown for $R=0$.²⁹ As seen in Figs. 1(a) and 1(b), noise smears out the transition into the synchronization region. The degrading effect of the noise is slightly less for larger noise correlation R but the difference between independent noise $R=0$ and common noise $R=1$ is small and only becomes detectable for rather strong noise. In Ref. 23 it is shown that common noise generates an effective coupling between the phases; therefore it degrades PS slightly less than uncorrelated noise.

We demonstrate quite different PS behavior in two coupled noisy chaotic Rössler oscillators,

$$\dot{x}_{1,2} = -\omega_{1,2}y_{1,2} - z_{1,2} + \epsilon(x_{2,1} - x_{1,2}), \quad (4)$$

$$\dot{y}_{1,2} = \omega_{1,2}x_{1,2} + 0.15y_{1,2} + D\xi_{1,2}(t), \quad (5)$$

$$\dot{z}_{1,2} = 0.4 + (x_{1,2} - 8.5)z_{1,2}, \quad (6)$$

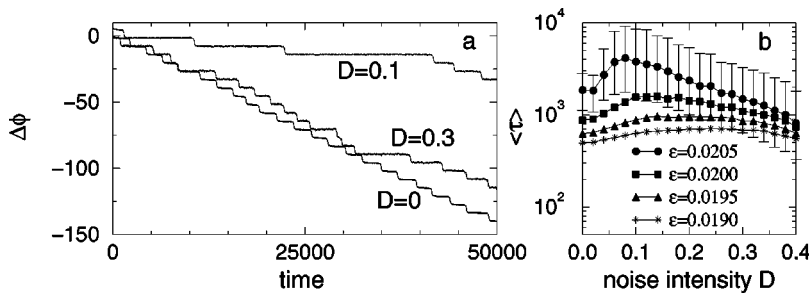


FIG. 2. Noise enhanced PS in two weakly coupled Rössler chaotic oscillators ($\epsilon=0.0205$). (a) Phase difference versus time for different noise intensity D . (b) Average duration of phase synchronization epochs versus noise intensity D for different coupling strength ϵ . The standard deviation is shown with error bars for $\epsilon=0.0205$.

with $\omega_1=0.99$ and $\omega_2=0.97$. For the chaotic Rössler oscillators, it is convenient to introduce amplitude and phase variables,⁵⁶ $A_i^2 = x_i^2 + y_i^2$ and $\tan \phi_i = y_i/x_i$. Chaotic fluctuation of A_i introduces a noiselike perturbation to the dynamics of phase difference $\Delta\phi$, and it has been shown that PS in chaotic oscillators resembles that in noisy periodic ones.^{15,56} In fact, at $D=0$, the transition point $\epsilon_{ps}=0.0208$ is somewhat higher than that of the periodic oscillators, as seen in Fig. 1.

In contrast to periodic oscillators, adding some noise to the chaotic oscillators can *enhance* PS significantly. For $D=0.1$ [Fig. 1(c)], $\Delta\Omega$ is considerably smaller than that for $D=0$ indicating enhanced PS below ϵ_{ps} ; above ϵ_{ps} there is a small nonvanishing $\Delta\Omega$ as a result of noise-induced intermittent phase slips.³⁰ For $D=0.3$ [Fig. 1(d)], $\Delta\Omega$ is larger than that for $D=0$ around ϵ_{ps} , however, it is clearly smaller in weaker coupling strength, indicating enhanced PS. Similar to periodic oscillators, PS has only a rather weak dependence on the noise correlation R . The difference between $R=0$ and $R=1$ is effectively invisible for $D=0.1$ and is small for $D=0.3$.

Figure 2(a) shows noise-enhanced PS for $\epsilon=0.0205$. At $D=0$, there are many epochs of phase synchronization between phase slips, and typically the epochs last for about 300 oscillation cycles. Adding a proper amount of noise to the two oscillators (e.g., $D=0.1$, $R=1$) prolongates remarkably the duration of the synchronization epochs: the two oscillators maintain PS for a period of about 3000 oscillation cycles. However, for stronger noise (e.g., $D=0.3$, $R=1$) phase slips again occur more frequently. To better characterize noise-enhanced PS, we focus on the mean duration $\langle\tau\rangle$ of the PS epochs. We find that $\langle\tau\rangle$ increases with the noise intensity D , reaches a maximal value and decreases for larger D for all coupling strengths analyzed [Fig. 2(b)]. The results are almost the same for independent noise $R=0$, but at large D , $\langle\tau\rangle$ takes slightly smaller values.

PS is essentially a phenomenon of adjusting time scales by weak interaction. To understand the constructive effect of noise on PS, we examine how noise changes time scales of chaotic oscillations. We calculate the return time T between two successive returns of the chaotic trajectory to a Poincaré section. There are many repetitive configurations of T as a result of the fact that there are many unstable periodic orbits (UPOs) embedded in the chaotic attractors⁵⁷ and chaotic trajectories can stay close to a certain UPO for some time. When adding a small amount of noise to the system, e.g., $D=0.1$, the repetition has been reduced considerably, because noise prevents the system from following the UPOs

closely for long time. Noise may also speed up or delay the return of the orbits, thus generates both small and large return times not presented in the noise-free systems.

Noise-enhanced PS in the two coupled Rössler oscillators can be explained through a consideration of the effect of noise on the UPOs. As in the case of periodically driven chaotic oscillators,^{58–60} PS of two coupled chaotic oscillators can be viewed as phase-locking of a number of pairs of UPOs. Those pairs with larger difference in time scales generally achieve locking at a larger coupling strength. All pairs of UPOs are mutually locked in the phase synchronization region. When the coupling strength is decreased past ϵ_{ps} , some pairs of UPOs become unlocked while others remain locked. In a pair of unlocked periodic orbits, the characteristic time for developing a phase slips has a dependence $\tau_{sl} \sim |\epsilon - \epsilon_{ps}|^{-1/2}$ as at typical type-I intermittency close to a saddle-node bifurcation.^{58–60} Phase slips of a chaotic oscillation now become possible, but only when the system comes to follow one of the unlocked pairs for at least a time of τ_{sl} long enough for a phase slip to occur. As illustrated in Fig. 3, the connection between phase slips and UPOs can be seen clearly for ϵ close to ϵ_{ps} where only a few pairs of UPOs become unlocked and it takes a rather long time τ_{sl} to complete a phase slip. Periodic orbits are manifested by almost vanishing $\Delta X_k = |X_{n+k} - X_n|$ which is the difference between the x variable at every k returns to the Poincaré section $y=0$, $x<0$, with a return time T_k . It is seen that phase slips occur between a period-4 UPO in oscillator 1 and a period-2 UPO in oscillator 2 which are followed closely by the systems for a fairly long time (~ 30 cycles). While most orbits are locked with return times fluctuating around a common value ($T=6.24$), these UPOs have clearly much smaller and larger return times [Figs. 3(e), 3(f)], thus remain unlocked by the coupling. With a noise of $D=0.1$, such a long time staying close to UPOs is rarely observed, and meanwhile most of the phase slips are eliminated (Fig. 2). At stronger noise, e.g., $D=0.4$ phase slips develop quickly when the oscillators come to some orbits with quite large differences in the return times, which cannot follow UPOs closely.

Thus we can explain the role of noise in PS of two coupled chaotic Rössler oscillators by two effects: (i) it prevents the system from staying close to the unlocked UPOs for long enough times to allow a phase slip to occur and (ii) it generates fluctuations in the return times and may induce phase slips of locked orbits as it does in coupled periodic orbits. The degree of PS is enhanced when (i) is dominant over (ii) at weak noise level, while it is degraded again when

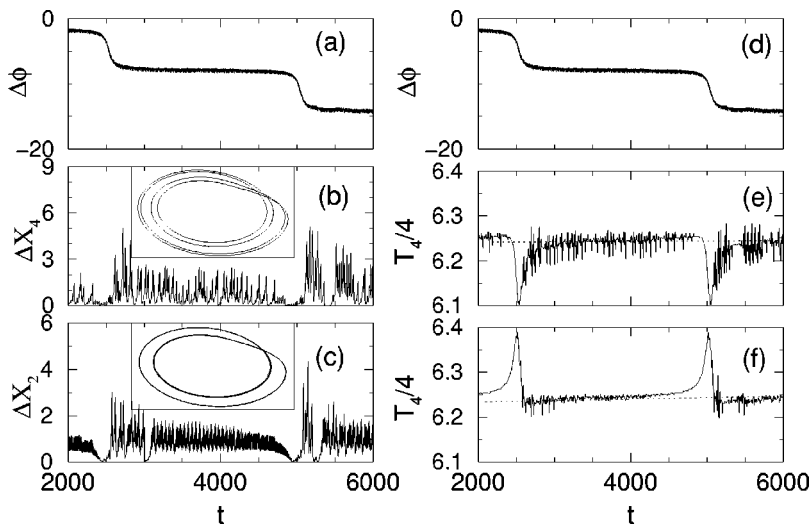


FIG. 3. Illustration of phase slips [(a),(d)] induced by unlocked UPOs [(b),(e) period-4 for oscillator 1; (c), (f), period-2 for oscillator 2] at $\epsilon=0.0205$. The insets in (b) and (c) show the unlocked UPOs around $t=2500$. Many locked UPOs can also be observed in this presentation.

(ii) becomes dominant at large noise. There thus exists an optimal noise intensity yielding the maximal enhancement as a result of the competition between these two factors. At a smaller coupling strength ϵ , more orbits become unlocked, and phase slips may develop already during a shorter time τ_{sl} when the oscillators approach some unlocked orbits. When noise prevents a phase slip, the trajectories may approach other unlocked orbits quickly; therefore, the enhancement of PS becomes less pronounced [Fig. 2(b)]. For ϵ well below ϵ_{ps} , phase slips occur frequently and are not always clearly associated to UPOs. Beyond ϵ_{ps} , only (ii) is active, and perfect PS is interrupted by noise-induced phase slips. Increasing correlation R of noise can slightly enhance PS further.

B. N globally coupled Rössler oscillators

In the following we consider an ensemble of N globally coupled nonidentical Rössler oscillators;

$$\dot{x}_i = -\omega_i y_i - z_i + \epsilon(X - x_i), \quad (7)$$

$$\dot{y}_i = \omega_i x_i + 0.15 y_i + D \xi_i, \quad (8)$$

$$\dot{z}_i = 0.4 + z_i(x_i - 8.5), \quad (9)$$

where $X = 1/N \sum_{i=1}^N x_i$ is the mean field. The parameters ω_i are randomly and uniformly distributed in $[\omega_0 - \delta, \omega_0 + \delta]$ with $\omega_0 = 1.0$ and $\delta = 0.025$.

For a small ensemble, e.g., $N=5$, we can see clearly a cascade of clustering of frequencies with the increase of coupling strength until global PS is achieved where all the oscillators are locked to a common frequency [Fig. 4(a)]. Close to the transition point of global synchronization, we can also observe a connection between phase slips and unlocked UPOs [Figs. 4(b) and 4(c)]. Although independent noise prevents the system from staying close to unlocked UPOs, it also induces phase slips among clustered oscillators. As a whole, we have not observed appreciable enhancement of PS of the ensemble by independent noise. A global noise can enhance PS, as will be seen also in a large ensemble below.

In a larger ensemble the transition to PS is much more complicated. The behavior of a set of $N=1000$ noisy chaotic oscillators is shown in Fig. 5.

We characterize the synchronization behavior of the ensemble by various quantities. The degree of PS can be characterized by the fluctuation amplitude of the mean field X .⁶¹ We calculate the variance $\sigma_X^2 = \langle X^2 \rangle_t - \langle X \rangle_t^2$ of X . Transition to PS can also be measured by frequency disorder σ_Ω which is defined by the standard deviation of the average frequency $\Omega_i = \langle \dot{\phi}_i \rangle$ of the oscillators in the ensemble. In the absence of noise, all the oscillators are locked to a common frequency and σ_Ω becomes zero at large enough coupling ϵ . However, a smaller σ_Ω may not always indicate a stronger degree of synchronization, especially in the clustering region where σ_Ω may not be small but the degree of synchronization is actually high. In the globally coupled ensemble, a transition to PS can also be quantitatively described by the mean order parameter² $\langle r(t) \rangle$ where $r(t) = |\sum_j \mathbf{P}_j(t)| / \sum_j |\mathbf{P}_j(t)|$.

$\mathbf{P}_j(t) = (x_j, y_j)$ are the state vectors in phase space at time t . The order parameter $\langle r(t) \rangle$ is zero for an infinite number of uncoupled oscillators and is one for strong coupling that yields complete or identical synchronization.

These quantities (σ_X^2 , σ_Ω , $\langle r(t) \rangle$), however, are not always suitable measures of the transition to PS, e.g., in locally coupled oscillators where phase locking of the oscillators and vanishing σ_Ω do not lead to clustering of the states

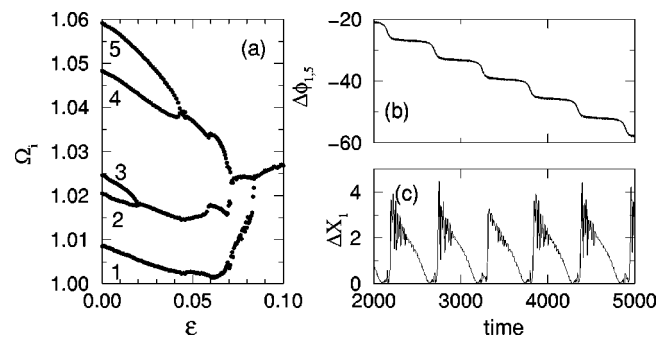


FIG. 4. (a) Transition to PS in the ensemble of $N=5$ globally coupled chaotic Rössler oscillators. A cascade of clustering of frequencies can be seen clearly. (b) Phase slips between oscillator 1 and 5 are generated by period-1 UPOs of oscillator 1, as seen by ΔX_1 in (c); $\epsilon=0.08$ is close to the threshold of global phase synchronization where the oscillators 2, 3, 4, and 5 have formed a cluster.

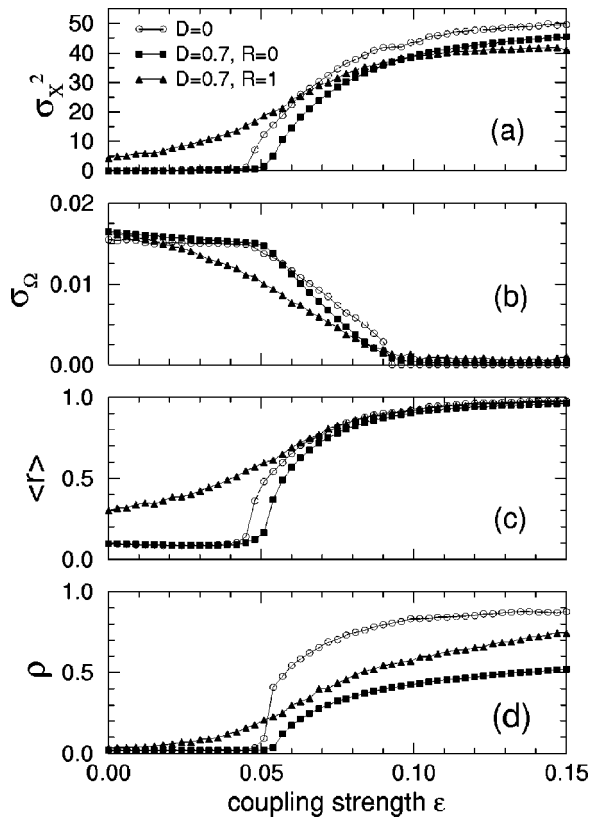


FIG. 5. Transition to PS in the ensemble of $N=1000$ globally coupled chaotic Rössler oscillators without or with noise.

in phase space due to the existence of waves, so that both σ_X^2 and $\langle r(t) \rangle$ are almost vanishing. We thus therefore for comparison purposes also measure the degree of PS based on temporal phase locking between the pairs of oscillators in the ensemble, which can be applied to systems with local coupling.⁶² The distribution of the cyclic relative phase difference $(\Delta\phi \bmod 2\pi)$ between an oscillator and a reference oscillator is constructed with a histogram of M bins.²⁹ Peaks

in the distribution show that there are preferred phase differences between the oscillators. The sharpness of the distribution characterizes the degree of phase synchronization, and is quantified by the entropy $S = -\sum_k^M p(k) \ln p(k)$.^{5,63} In the ensemble, we randomly choose an oscillator as a reference oscillator and compute the entropy $S(i)$ of the i th oscillator with respect to the reference one. By averaging over the ensemble and normalizing with the entropy of the uniform distribution $S_m = \ln(M)$, we get the PS index,

$$\rho = (S_m - \langle S \rangle) / S_m. \quad (10)$$

ρ shows no sensitive dependence on the reference oscillator. The PS degree is higher for larger ρ . Note that in coupled chaotic oscillators, the phase difference fluctuates around a constant value even in the perfect phase locking region. As a result, $\rho < 1$.

As seen in Fig. 5, in the noise-free ensemble, all the measures vary slowly until $\epsilon \approx 0.043$ where they start to change quickly and finally global PS is achieved at $\epsilon_{ps} \approx 0.093$. In the crossover region $0.043 < \epsilon < 0.093$, many oscillators are locked into a single cluster with a common frequency while the others still have distributed frequencies. A macroscopic oscillation emerges and its amplitude increases with ϵ as more oscillators become phase locked. One can see that the dependence of $\langle r(t) \rangle$ on the coupling strength is closely related to that of σ_X^2 .

PS is degraded when independent noise ($R=0$) is added to the ensemble as seen by smaller σ_X^2 and ρ . (This is in contrast to the behavior of the two oscillator systems.) In the crossover region, σ_Ω is smaller than that of the noise-free ensemble; however, this does not lead to increased PS. ρ becomes smaller than that at $D=0$. In contrast, a global noise ($R=1$) can enhance PS in the weak coupling regime: σ_Ω is considerably smaller, and σ_X^2 and ρ are clearly larger than those in the absence of noise.

Typical behavior of the ensemble in the weak coupling region is shown in Fig. 6 for different intensities of global noise ($R=1$) at $\epsilon=0.045$. Without noise, there is no clear

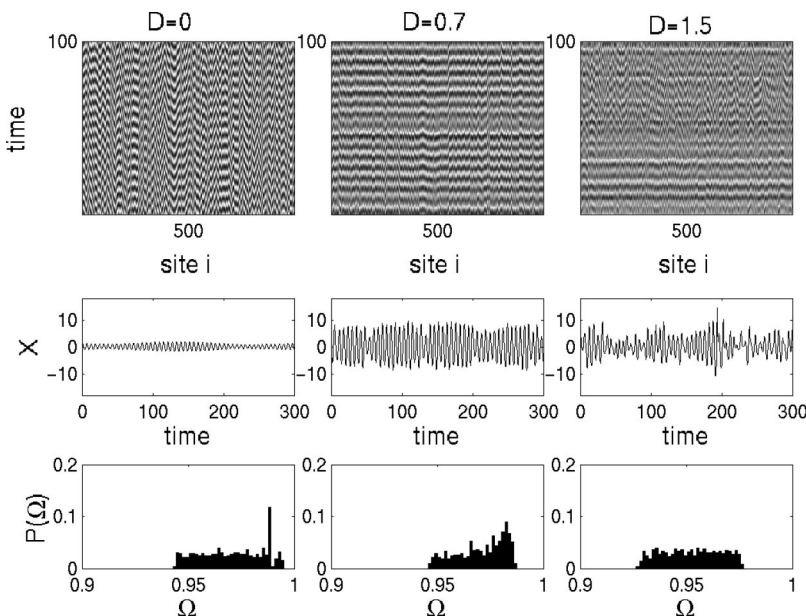


FIG. 6. Synchronization behavior of an ensemble of $N=1000$ globally coupled ($\epsilon=0.045$) chaotic Rössler oscillators with a global noise of various intensities. Upper panel: space-time plot of y_i in gray scales (with white representing maximal and black minimal values); Middle panel: the corresponding mean field X versus time. Lower panel: the corresponding distributions of average frequency Ω_i of the oscillators.

synchronization behavior over the whole ensemble; however, clustering of some of the oscillators can be observed from the space–time plot of the states, as well as in the distribution of the average frequency Ω_i of the oscillators. The mean field X displays oscillations with rather small amplitudes due to the clustering of some oscillators. Adding a global noise with $D=0.7$ makes the whole ensemble achieve pronounced synchronization and generate a coherent collective oscillation, although perfect phase locking of those clustered oscillators is spoiled. The frequency of more oscillators shifts to distribute around the clustering frequency. At a stronger noise intensity $D=1.5$, the phase dynamics of individual oscillators becomes quite incoherent and synchronization is lost frequently. The mean field X still has large amplitudes but its temporal behavior is rather noisy. The distribution of frequency also becomes broad and moves to smaller values because the trajectories of oscillators in the presence of large noise can approach quite closely to the unstable fixed point around $(x,y)=(0,0)$ where the oscillations slow down.

Now we have seen clearly that global noise plays a significant role in phase synchronization of weakly coupled chaotic oscillators. The ensemble establishes the most coherent collective oscillation at a certain intermediate noise intensity. To characterize the coherence of the ensemble, we focus on the time series of the mean field X . Its amplitude and temporal coherence reflect the degree of synchronization and temporal coherence in the lattice, respectively. A combination measure of the spatio-temporal coherence based on X can be defined as³⁷

$$\beta = H \frac{\Omega_p}{\Delta\Omega}, \quad (11)$$

where Ω_p is the frequency of the main peak in the spectrum of X , H is the peak height mainly depending on the amplitude of X , and $\Delta\Omega$ is the half-width of the peak reflecting temporal randomness of X .

In Fig. 7 computed values of β obtained from simulations are shown along with the variance of the mean field X and the phase synchronization index ρ , as a function of the intensity D of global noise for various coupling strengths in the weak coupling region. We find that when the oscillators are not coupled ($\epsilon=0$), the global noise alone leads to a slight enhancement of PS as seen by increasing σ_X^2 and $\langle r \rangle$; however, the degree of PS is rather low: ρ increases slightly but remains small. Fairly strong noise can induce a visible macroscopic mean field, but the coherence β has only small values. Phase synchronization between uncoupled oscillators induced by a common noise has also been investigated,²³ where it is shown that the systematic contribution from the common noise is equivalent to an effective coupling between the phases. If a weak coupling is introduced (e.g., $\epsilon=0.045$ which is below ϵ_{ps}) the interplay between the global noise and weak coupling is able to achieve some PS. The combination of rather weak coupling and noise generates a coherent collective motion in the ensemble. The system clearly displays a resonant behavior; with an increase of noise intensity the coherence β of the collective oscillation increases, reaches a maximum, and decreases at large noise intensity, displaying the typical feature of the CR.^{35–37,41,42}

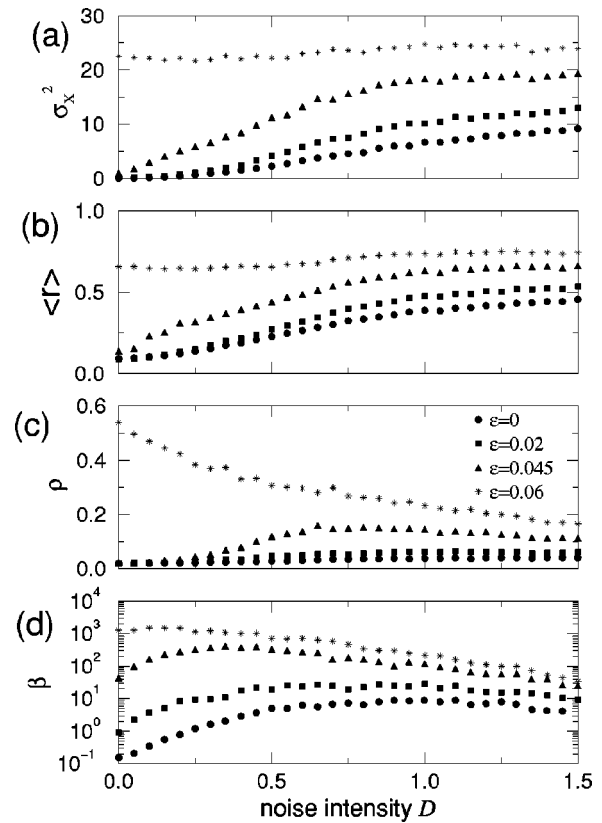


FIG. 7. Coherence resonance features of the ensemble in the weak coupling regime. (a) The variance σ_X^2 of the mean field X ; (b) order parameter $\langle r \rangle$; (c) phase synchronization index ρ ; and (d) the coherence factor β of X .

A more detailed examination of the peak height H and the quality factor $\Omega_p/\Delta\Omega$ in Eq. (11) for $\epsilon=0.045$ shows that at weak noise intensities H increases quickly and the quality factor varies slightly, as seen in Fig. 8. Thus weak

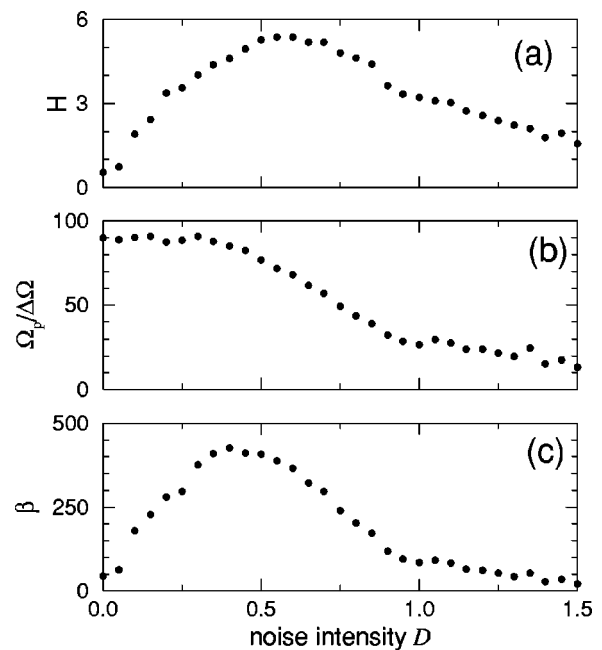


FIG. 8. Dependence on noise intensity of H , $\Omega_p/\Delta\Omega$, and the coherence factor β [see Eq. (11)]; $\epsilon=0.045$.

global noise enhances synchronization clearly, while the oscillations of individual oscillators remain coherent. At large noise intensities, the trajectories can come rather close to the fixed point around $(x, y) = (0, 0)$, and the oscillations become more incoherent. Both H and $\Omega_p / \Delta\Omega$ decrease, resulting in a quick decrease of β . The coherence resonance feature in the weak coupling regime thus is a consequence of a competition between noise-enhanced PS and noise-induced incoherence in the oscillations. The optimal noise intensity of the maximal coherence moves to smaller values with increasing ϵ until the region of pronounced phase synchronization where noise acts to degrade PS and coherence (e.g., at $\epsilon = 0.06$). Unlike the case of two coupled chaotic oscillators, enhanced PS in populations is mainly due to interplay between actual global coupling and the effective coupling resulting from the common component of noise. For fixed noise intensity D , the degree of PS and coherence decreases with the noise correlation R .

III. EXPERIMENTAL RESULTS

We have also carried out experiments on noise enhanced PS with two and sixty-four weakly coupled chaotic electrochemical oscillators. The reaction used is the electrodisolution of nickel in sulfuric acid solution. The oscillations in this and many other electrochemical systems⁶⁴ result from the interaction of a (hidden) negative differential resistance of the faradaic process with potential drops in the electrolyte and/or in external resistances and with (normally slower) reaction and transport steps. By changing parameters such as applied potential, external resistance, electrolyte concentration, and cell geometry steady, periodic, and chaotic behavior can be found. The reaction takes place on individual reacting sites (electrodes) and the current, proportional to the rates of dissolution, can be independently measured. Such systems constitute a good platform for the study of coupled chaotic oscillators.

A. Experimental setup

A schematic of the experimental apparatus is shown in Fig. 9. A standard electrochemical cell consisting of nickel working electrode array (64 1 mm diam electrodes in 8×8 geometry with 2 mm spacing; the two electrode experiments are done with only two elements in the array with a distance of 18 mm), a Hg/Hg₂SO₄/cc.K₂SO₄ reference electrode, and a platinum mesh counter electrode is used. The potential of all electrodes is held at the same value $V = V_0 + D\xi$, where V_0 is an offset potential, D is the noise intensity and ξ is a Gaussian noise with zero mean and a standard deviation of 1. Thus in the experiments the applied noise is common; $R = 1$ in Eq. (1). The currents of electrodes are measured independently at a sampling rate of 100 Hz. The experiments are carried out in 4.5 M sulfuric acid electrolyte at a temperature of 11 °C.

The electrodes are connected to the potentiostat through individual parallel resistors, R_{ind} , and through one collective series resistors, R_{coll} (see Fig. 9). The collective resistor couples the electrodes globally; the coupling strength is characterized by the fraction of collective resistance, $\epsilon = R_{\text{coll}} / R_{\text{tot}}$, where $R_{\text{tot}} = R_{\text{coll}} + R_{\text{ind}} / N$. For $\epsilon = 0$, the exter-

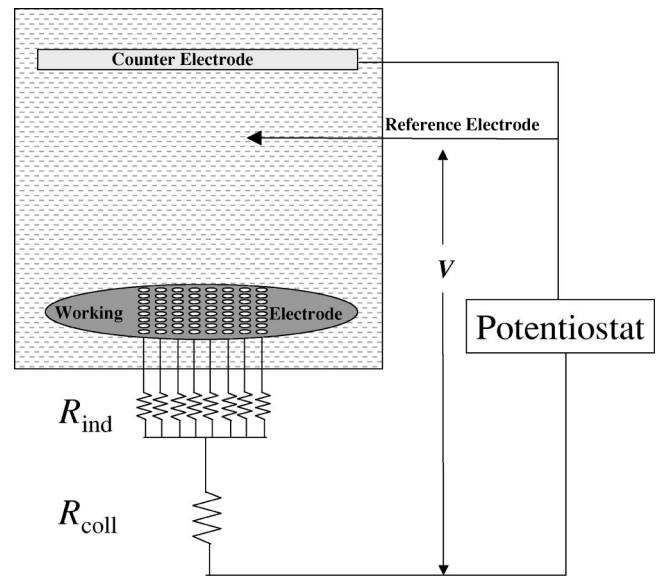


FIG. 9. Schematic of the experimental setup.

nal resistance furnishes no additional global coupling, for $\epsilon = 1$ maximum external global coupling is achieved.

B. Results

1. Dynamics of a single element

We start with a description of the dynamics of the reaction of a single reaction site, i.e., on a single electrode; details can be found in a previous publication.⁶⁵ A chaotic time series of a single oscillator is shown in Fig. 10(a); the chaos is reached via a period-doubling bifurcation sequence as the applied potential is changed. The chaotic attractor [Fig. 10(b), reconstructed from the current by the use of the time delays] is low-dimensional; the information dimension of the attractor is $D_1 = 2.3 \pm 0.1$.⁵⁰ The power spectrum [Fig. 10(a), inset] is broad with a dominant peak at $f = 1.270$ Hz. The instantaneous phase and amplitude are obtained with the Hilbert transform;⁵⁶ the dc component of the current is eliminated [$I(t) = i(t) - i_{\text{mean}}$] [phase portrait, Fig. 10(c)]. To increase the robustness of the phase analysis the origin is moved to the square shown in Fig. 10(c). The phase ($\phi(t)$) and the amplitude ($A(t)$) are obtained from the angle and the length of the phase point, respectively, in Fig. 10(c) at time t . In Fig. 10(d) the phase is shown as a function of time; some small deviations from the straight line arises because of the chaotic nature of the signal. The frequency is calculated from the slope,

$$\Omega = \frac{1}{2\pi} \left\langle \frac{d\phi}{dt} \right\rangle. \quad (12)$$

The frequency of a single element has been found to be $\omega = 1.275$ Hz, which is close to the dominant peak in the power spectrum.

2. The dynamics of two elements

In the experiments described here the inherent coupling (through the electrolyte) is very weak. In a two electrode setup without added coupling a small frequency mismatch

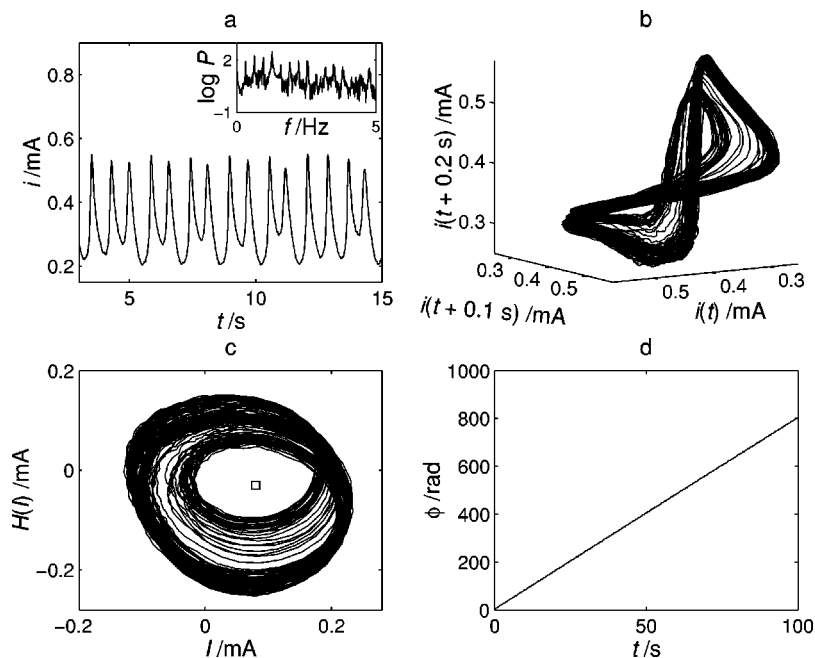


FIG. 10. Chaotic dynamics of a single element. $V_0 = 1.310$ V, $R = 908$ Ω . (a) Time series of current and the power spectrum (inset). (b) Reconstructed attractor using time delay coordinates. (c) Phase portrait obtained with Hilbert transform. (d) Phase versus time.

(about $\Delta\omega = 14$ mHz) can be obtained because of surface heterogeneities. With added weak coupling phase synchronization occurs at about $\epsilon_{ps} = 0.08$; the frequencies of the oscillators become equal and the distribution of the phase differences has a large maximum around $\Delta\phi = 0$. We first analyze the dynamics just below ϵ_{ps} and then show the constructive effect of common noise on phase synchronization.⁴⁸

At $\epsilon = 0.06$, i.e., just below ϵ_{ps} , the observed frequency mismatch ($\Delta\Omega = 5$ mHz) is smaller than that seen without coupling, however, the coupling is not strong enough for phase synchronization. During the time of the experiment one phase slip was observed as seen in Fig. 11(a). The analysis of the time series of the two oscillators shows that the phase slip occurs when both oscillators approach the neighborhood of an unlocked period-3 UPO. In Fig. 11(b) the ΔX_3 values are shown as a function of time for the two oscillators. The coincidence of the approach of unlocked UPOs and the phase slip confirms the numerical predictions about the dynamics close to but below ϵ_{ps} .

We investigate noise enhanced PS at a somewhat lower coupling strength: $\epsilon = 0.04$. [In general the enhancement is seen at values of ϵ not close to ϵ_{ps} ; this was seen in the simulations, e.g., Fig. 1(d).] During the time of the experiment (about 200 oscillations) there are two phase slips between the oscillators [see Fig. 12(a)] corresponding to a frequency difference $\Delta\Omega = 12$ mHz. As can be seen in Figs. 12(a)–12(c) the first phase slip can be attributed to the unlocked period-4 UPOs. The synchronization time τ_{sl} during the phase slip is much shorter than that for $\epsilon = 0.06$. We see that the phase slips occur more frequently and develop more quickly than at the stronger coupling strengths. Moreover, the second phase slip cannot be clearly linked to UPOs. These observations are also in agreement with the numerical calculations obtained further from ϵ_{ps} . By adding a small amount of zero-mean Gaussian noise (the standard deviation is 3×10^{-4} V measured at 200 Hz) to the (common) poten-

tial of the electrodes we get a qualitatively different synchronization behavior. With this small noise, the deterministic nature of the electrodisolution process is still dominant; the reconstructed attractors (not shown) resemble those without noise. However, the phase slips are eliminated and the phase difference fluctuates around zero [Fig. 12(d)]. The oscillators do not have as long time of residence close to UPSs [Figs. 12(e) and 12(f)] as in the noise-free case. The absence of phase slips during the 200 oscillations of the experiment is consistent with the model calculations which predict lengths of the phase synchronized epochs on the order of a thousand oscillations.

Experiments have also been carried out with weaker added coupling, $\epsilon = 0.02$ and 0. No phase synchronization was obtained with noise up to an intensity at which the oscillators exhibited (noisy) periodic dynamics. With smaller electrode spacing and thus greater inherent coupling (4 mm rather than 18 mm as above) the added noise is able to

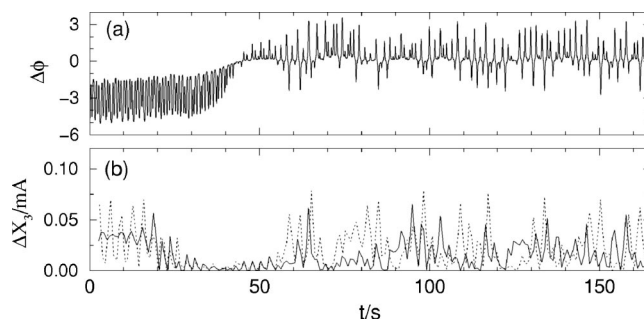


FIG. 11. Two coupled ($\epsilon = 0.06$) chaotic elements just below $\epsilon_{ps} = 0.08$. $R_{tot} = 330$ Ω , $V_0 = 1.280$ V. (a) Phase difference between the two oscillators versus time. (b) The difference between the next return values of the current maxima ($\Delta X_3 = |X_n - X_{n-3}|$, where X_n is the n th maximum) of the two oscillators (solid: oscillator 1; dashed: oscillator 2) as a function of time.

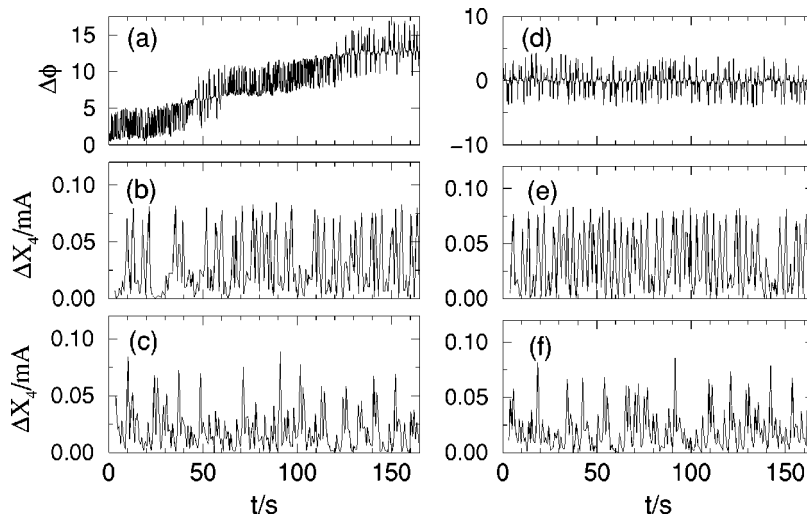


FIG. 12. Two coupled ($\epsilon=0.04$) chaotic oscillators without [left panel, (a)–(c)] and with [right panel, (d)–(f)] small amounts of common, zero-mean Gaussian noise (standard deviation of 3×10^{-4} V measured at 200 Hz). Top row: phase difference between the oscillators versus time. Middle and bottom rows: the difference between the next return values of the maxima of the oscillators, $\Delta X_4 = |X_n - X_{n-4}|$, (middle: oscillator 1, bottom: oscillator 2) versus time. $R_{\text{tot}}=500 \Omega$, $V_0=1.350$ V.

achieve phase synchronization of the oscillators with less added coupling, $\epsilon=0.02$.

3. Sixty four electrodes

Consider now a population of chaotic oscillators. To explore the effect of noise on the dynamics we have carried out experiments without ($\epsilon=0$) and with very weak ($\epsilon=0.014$) global coupling and changed the noise intensity D . The detailed results are shown only for $\epsilon=0.014$. In Fig. 13(a), the typical time series of one element in the array is shown with the power spectrum. They are similar to those of a single element [see Fig. 10(a)]. The space–time plot of the elements does not show any obvious sign of synchronization.

The elements in the array exhibit some variation again, there is a distribution of frequencies [Fig. 13(d)] and phases [Fig. 13(e)]. The variations of the mean field time series [i.e., mean current, $h(t)=1/N \sum_k i_k(t)$] are small [Fig. 13(b)]. Thus, there is only very small coherence; the coupling is not strong enough for phase synchronization.

Next we show the effect of added noise. If the noise intensity is small ($D=4$ mV, Fig. 14) there is only a slight change in the dynamics of the individual elements, however, the collective behavior changes dramatically. The space–time plot shows more ordered behavior and the frequency of 50 oscillators become equal, and many oscillators have similar phase. There is a larger variation of the mean field and the

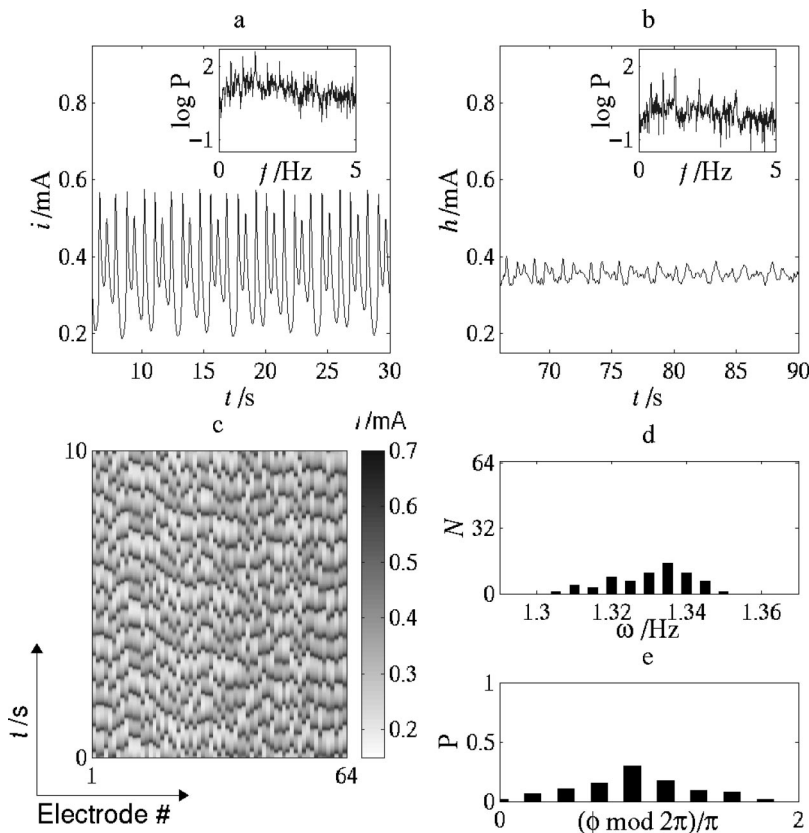


FIG. 13. Dynamics of sixty four electrodes at $\epsilon=0.014$ without noise, $D=0$ mV. (a) Representative time series of a current of individual element (inset: the corresponding power spectrum). (b) Mean field time series and its power spectrum (inset). (c) Space–time plot of individual currents. (d) Frequency distribution. (e) Histogram of phases at $t=50$ s.

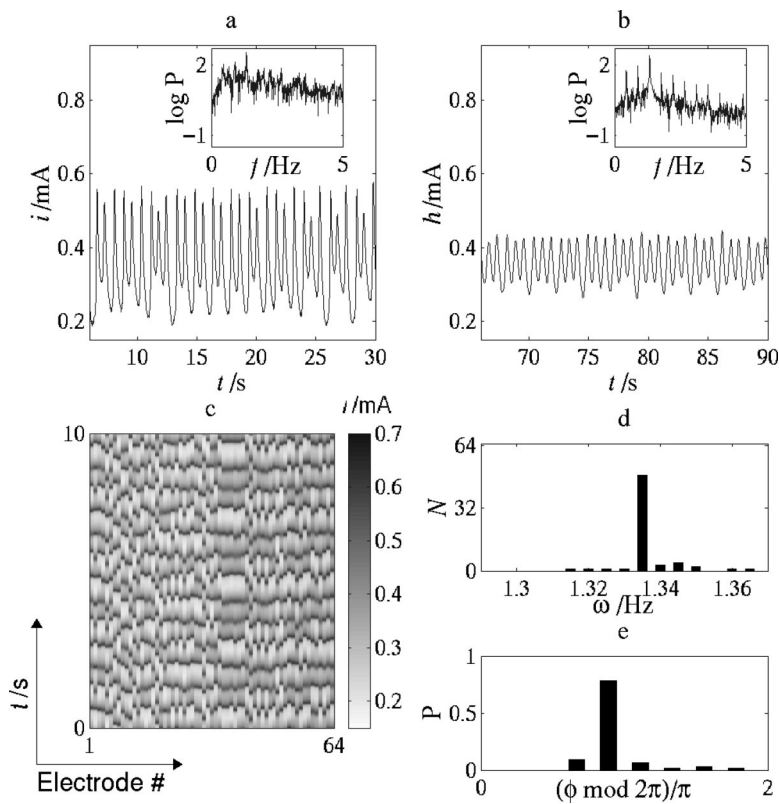


FIG. 14. Dynamics with optimal noise intensity, $D = 4$ mV, $\epsilon = 0.014$. (a) Representative time series of a current of individual element (inset: the corresponding power spectrum). (b) Mean field time series and its power spectrum (inset). (c) Space-time plot of individual currents. (d) Frequency distribution. (e) Histogram of phases at $t = 50$ s.

power spectrum of the mean field exhibits a strong peak at the dominant frequency. Thus, this small noise intensity induced coherent behavior. With increasing the noise intensity ($D = 10$ mV, Fig. 15) the coherent motion of the mean field

breaks down, the frequency distribution becomes larger, and the phases become more scattered.

We have calculated five measures to characterize the collective behavior of the oscillators: the variance of the mean

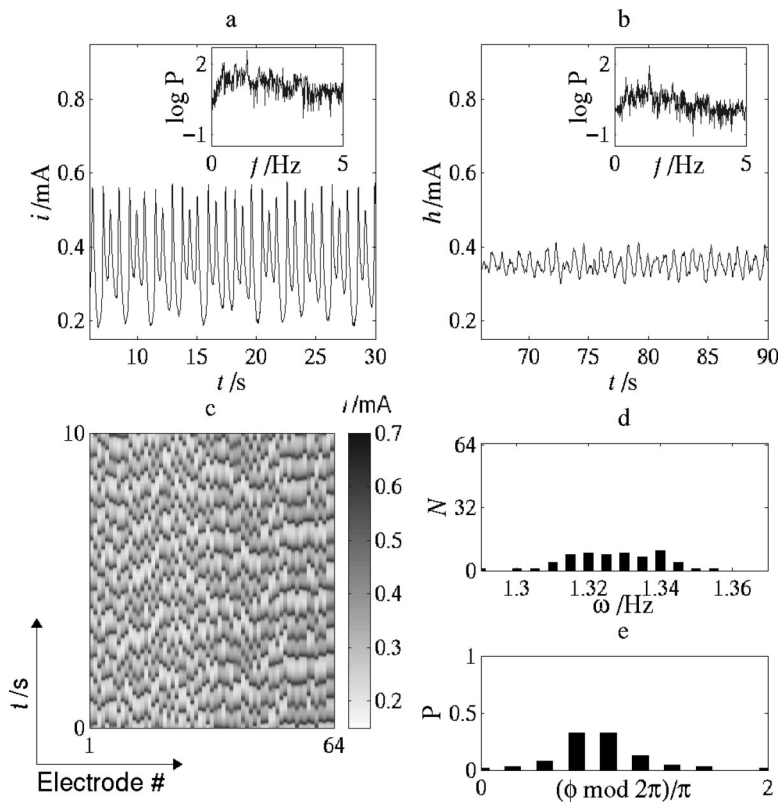


FIG. 15. Dynamics with excessive noise, $D = 10$ mV, $\epsilon = 0.014$. (a) Representative time series of a current of individual element (inset: the corresponding power spectrum). (b) Mean field time series and its power spectrum (inset). (c) Space-time plot of individual currents. (d) Frequency distribution. (e) Histogram of phases at $t = 50$ s.

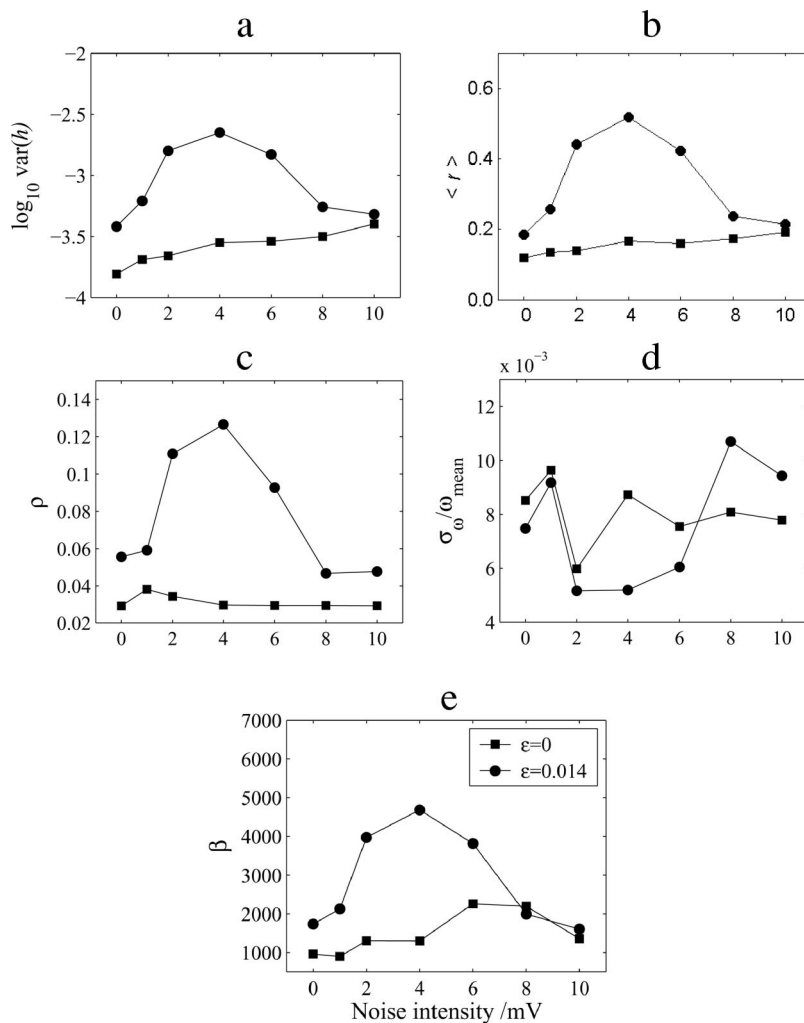


FIG. 16. Different measures of collective behavior as a function of noise intensity for $\epsilon=0$ (squares) and 0.014 (circles). (a) Variance of mean field. (b) Order parameter. (c) Temporal phase synchronization index. (d) Relative standard deviation of frequencies. (e) Coherence factor.

field $\text{var}(h)$, the order parameter $\langle r \rangle$, the temporal phase synchronization index ρ , the coherence factor β , and the standard deviation of the frequencies of the elements, $\sigma_{\omega}/\omega_{\text{mean}}$. These are shown as a function of the noise intensity in Fig. 16 for $\epsilon=0$ and 0.014. It is seen that the coherence resonance is stronger at $\epsilon=0.014$ than at 0. The variance of mean field and the order parameter increase in a monotone way for $\epsilon=0$, but shows a maximum for $\epsilon=0.014$. The resonance behavior can also be observed in ρ and β —there is small variation for $\epsilon=0$ and a resonance curve for $\epsilon=0.014$. However, the frequency distribution [Fig. 16(d)] does not clearly show the trend above; although for $\epsilon=0.014$ there is a minimum at optimal noise intensity, for $\epsilon=0$ there are larger variations.

The experiments on sets of globally coupled chaotic oscillators confirm the noise induced effects predicted by numerical calculations. At an optimal common noise intensity increased measure of phase synchronization and coherent oscillations are observed; the effects are stronger with weak inherent coupling.

IV. DISCUSSION

We have demonstrated both in numerical simulations and in laboratory experiments that noise can play a constructive role in the enhancement of phase synchronization of

weakly coupled chaotic oscillators. In a system of two weakly coupled chaotic oscillators, phase slips are associated with unlocked UPOs close to the threshold of synchronization and noise enhances PS because it prevents the system from staying close to the unlocked UPOs. The interplay between noise and UPOs plays a constructive role in PS. This is in contrast to the behavior close to the threshold of CS in coupled identical chaotic systems. In the latter case there are many transversely unstable UPOs (Refs. 18,20) and the synchronization error can be amplified from the noise level to generate bursts of desynchronization by these UPOs even in the presence of extremely weak independent noise components η .^{17,19}

Enhanced phase synchronization has also been seen in a population of globally coupled oscillators with common noise. At intermediate noise strengths coherent macroscopic oscillations of the mean field are observed; excessive noise breaks up the coherent behavior. The system displays coherence resonance as a result of the competition between noise-enhanced PS and noise-induced incoherence of phase dynamics.

The mechanism of CR of coupled oscillatory elements is different from that in excitable systems^{35–37} or in switching between coexisting attractors.^{41,42} The noise-enhanced phase synchronization described in this paper is caused by a differ-

ent mechanism from that occurring in excitable media subjected to spatially uncorrelated noise.^{45,46,66}

Our finding is of significance for understanding the cooperative effects of noise and weak coupling in different physical, chemical, and biological systems. For example, in ecology, environmental fluctuations may play a role in synchronization of population oscillations over large geographical regions.^{67–70}

ACKNOWLEDGMENTS

This work was supported by the National Science Foundation (CTS-0000483) and the Office of Naval Research (N00014-01-1-0603), the Humboldt Foundation, the European Community (HPRN-CT-2000-00158), and the Deutsche Forschungsgemeinschaft (SFB 555). We acknowledge the Max Planck Institut für Physik Komplexer Systeme for support during the Seminar on Control, Communication, and Synchronization in Chaotic Dynamical Systems (Oct. 14–Nov. 23, 2001).

- ¹A. T. Winfree, *The Geometry of Biological Time* (Springer-Verlag, New York, 1980).
- ²Y. Kuramoto, *Chemical Oscillations, Waves, and Turbulence* (Springer, Berlin, 1984).
- ³V. S. Anishchenko, A. G. Balanov, N. B. Janson, N. B. Igosheva, and G. V. Borduygov, *Int. J. Bifurcation Chaos Appl. Sci. Eng.* **10**, 2339 (2000).
- ⁴C. Schäfer, M. G. Rosenblum, H. H. Abel, and J. Kurths, *Phys. Rev. E* **60**, 857 (1999).
- ⁵P. Tass, M. G. Rosenblum, J. Weule, J. Kurths, A. Pikovsky, J. Volkmann, A. Schnitzler, and H. J. Freund, *Phys. Rev. Lett.* **81**, 3291 (1998).
- ⁶A. Neiman, X. Pei, D. Russell, W. Wojtenek, L. Wilkens, F. Moss, H. A. Braun, M. T. Huber, and K. Voigt, *Phys. Rev. Lett.* **82**, 660 (1999).
- ⁷R. C. Elson, A. I. Selverston, R. Huerta, N. F. Rulkov, M. I. Rabinovich, and H. D. I. Abarbanel, *Phys. Rev. Lett.* **81**, 5692 (1998).
- ⁸T. L. Carroll, J. F. Heagy, and L. M. Pecora, *Phys. Rev. E* **54**, 4676 (1996).
- ⁹R. A. Oliva and S. H. Strogatz, *Int. J. Bifurcation Chaos Appl. Sci. Eng.* **11**, 2359 (2001).
- ¹⁰R. A. York and R. C. Compton, *IEEE Trans. Microwave Theory Tech.* **39**, 1000 (1991).
- ¹¹I. Z. Kiss, Y. M. Zhai, and J. L. Hudson, *Science* **296**, 1676 (2002).
- ¹²A. S. Pikovsky and P. Grassberger, *J. Phys. A* **24**, 4587 (1991).
- ¹³L. M. Pecora and T. L. Carroll, *Phys. Rev. Lett.* **64**, 821 (1990).
- ¹⁴H. Fujisaka and T. Yamada, *Prog. Theor. Phys.* **69**, 32 (1983).
- ¹⁵M. G. Rosenblum, A. S. Pikovsky, and J. Kurths, *Phys. Rev. Lett.* **76**, 1804 (1996).
- ¹⁶S. Boccaletti, J. Kurths, G. Osipov, D. L. Valladares, and C. S. Zhou, *Phys. Rep.* **366**, 1 (2002).
- ¹⁷C. S. Zhou and C. H. Lai, *Phys. Rev. E* **59**, R6243 (1999).
- ¹⁸D. J. Gauthier and J. C. Bienfang, *Phys. Rev. Lett.* **77**, 1751 (1996).
- ¹⁹A. Cenys and H. Lustfeld, *J. Phys. A* **29**, 11 (1996).
- ²⁰J. F. Heagy, T. L. Carroll, and L. M. Pecora, *Phys. Rev. E* **52**, R1253 (1995).
- ²¹R. V. Jensen, *Phys. Rev. E* **58**, R6907 (1998).
- ²²A. S. Pikovsky, *Radiophys. Quantum Electron.* **27**, 576 (1984).
- ²³C. S. Zhou and J. Kurths, *Phys. Rev. Lett.* **88**, 230602 (2002).
- ²⁴R. Toral, C. R. Mirasso, E. Hernandez-Garcia, and O. Piro, *Chaos* **11**, 665 (2001).
- ²⁵C. H. Lai and C. S. Zhou, *Europhys. Lett.* **43**, 376 (1998).
- ²⁶A. S. Pikovsky, *Phys. Lett. A* **165**, 33 (1992).
- ²⁷A. S. Matsumoto and I. Tsuda, *J. Stat. Phys.* **31**, 87 (1983).
- ²⁸A. B. Neiman and D. F. Russel, *Phys. Rev. Lett.* **88**, 138103 (2002).
- ²⁹R. L. Stratonovich, *Topics in the Theory of Random Noise* (Gordon and Breach, New York, 1967).
- ³⁰L. Q. Zhu, A. Raghu, and Y. C. Lai, *Phys. Rev. Lett.* **86**, 4017 (2001).
- ³¹R. Benzi, A. Sutera, and A. Vulpiani, *J. Phys. A* **14**, L453 (1981).
- ³²K. Wiesenfeld and F. Moss, *Nature (London)* **373**, 33 (1995).
- ³³L. Gammaitoni, P. Hänggi, P. Jung, and F. Marchesoni, *Rev. Mod. Phys.* **70**, 223 (1998).
- ³⁴A. Neiman, A. Silchenko, V. Anishchenko, and L. Schimansky-Geier, *Phys. Rev. E* **58**, 7118 (1998).
- ³⁵A. S. Pikovsky and J. Kurths, *Phys. Rev. Lett.* **78**, 775 (1997).
- ³⁶A. Longtin, *Phys. Rev. E* **55**, 868 (1997).
- ³⁷H. Gang, T. Ditzinger, C. Z. Ning, and H. Haken, *Phys. Rev. Lett.* **71**, 807 (1993).
- ³⁸L. Gammaitoni, F. Marchesoni, and S. Santucci, *Phys. Rev. Lett.* **74**, 1052 (1995).
- ³⁹B. Shulgin, A. Neiman, and V. Anishchenko, *Phys. Rev. Lett.* **75**, 4157 (1995).
- ⁴⁰J. A. Freund, A. B. Neiman, and L. Schimansky-Geier, *Europhys. Lett.* **50**, 8 (2000).
- ⁴¹C. Palenzuela, R. Toral, C. R. Mirasso, O. Calvo, and J. D. Gunton, *Europhys. Lett.* **56**, 347 (2001).
- ⁴²C. Masoller, *Phys. Rev. Lett.* **88**, 034102 (2002).
- ⁴³S. Kádár, J. C. Wang, and K. Showalter, *Nature (London)* **391**, 770 (1998).
- ⁴⁴H. Hempel, L. Schimansky-Geier, and J. Garcia-Ojalvo, *Phys. Rev. Lett.* **82**, 3713 (1999).
- ⁴⁵B. B. Hu and C. S. Zhou, *Phys. Rev. E* **61**, R1001 (2000).
- ⁴⁶C. S. Zhou, J. Kurths, and B. Hu, *Phys. Rev. Lett.* **87**, 098101 (2001).
- ⁴⁷D. E. Postnov, S. K. Han, T. G. Yim, and O. V. Sosnovtseva, *Phys. Rev. E* **59**, R3791 (1999).
- ⁴⁸C. S. Zhou, J. Kurths, I. Z. Kiss, and J. L. Hudson, *Phys. Rev. Lett.* **89**, 014101 (2002).
- ⁴⁹I. Z. Kiss and J. L. Hudson, *Phys. Rev. E* **64**, 046215 (2001).
- ⁵⁰I. Z. Kiss, W. Wang, and J. L. Hudson, *Phys. Chem. Chem. Phys.* **2**, 3847 (2000).
- ⁵¹W. Wang, I. Z. Kiss, and J. L. Hudson, *Chaos* **10**, 248 (2000).
- ⁵²W. Wang, I. Z. Kiss, and J. L. Hudson, *Phys. Rev. Lett.* **86**, 4954 (2001).
- ⁵³Z. F. Mainen and T. J. Sejnowski, *Science* **268**, 1503 (1995).
- ⁵⁴A. C. Tang, A. M. Bartels, and T. J. Sejnowski, *Cereb. Cortex* **7**, 502 (1997).
- ⁵⁵P. A. P. Moran, *Aust. J. Zool.* **1**, 291 (1953).
- ⁵⁶A. S. Pikovsky, M. G. Rosenblum, G. V. Osipov, and J. Kurths, *Physica D* **104**, 219 (1997).
- ⁵⁷E. Ott, *Chaos in Dynamical Systems* (Cambridge University Press, Cambridge, 1993).
- ⁵⁸A. Pikovsky, G. Osipov, M. Rosenblum, M. Zaks, and J. Kurths, *Phys. Rev. Lett.* **79**, 47 (1997).
- ⁵⁹A. Pikovsky, M. Zaks, M. Rosenblum, G. Osipov, and J. Kurths, *Chaos* **7**, 680 (1997).
- ⁶⁰M. A. Zaks, E. H. Park, M. G. Rosenblum, and J. Kurths, *Phys. Rev. Lett.* **82**, 4228 (1999).
- ⁶¹A. S. Pikovsky, M. G. Rosenblum, and J. Kurths, *Europhys. Lett.* **34**, 165 (1996).
- ⁶²C. S. Zhou and J. Kurths, *Phys. Rev. E* **65**, 040101(R) (2002).
- ⁶³C. Schäfer, M. G. Rosenblum, J. Kurths, and H. H. Abel, *Nature (London)* **392**, 239 (1998).
- ⁶⁴M. T. M. Koper, *Adv. Chem. Phys.* **92**, 161 (1996).
- ⁶⁵I. Z. Kiss, Y. Zhai, and J. L. Hudson, *Ind. Eng. Chem. Res.* (in press).
- ⁶⁶A. Neiman, L. Schimansky-Geier, A. Cornell-Bell, and F. Moss, *Phys. Rev. Lett.* **83**, 4896 (1999).
- ⁶⁷O. N. Bjørnstad, R. A. Ims, and X. Lambin, *Trends Ecol. Evol.* **14**, 427 (1999).
- ⁶⁸P. J. Hudson and I. M. Cattadori, *Trends Ecol. Evol.* **14**, 1 (1999).
- ⁶⁹W. D. Koenig, *Trends Ecol. Evol.* **14**, 22 (1999).
- ⁷⁰B. Cazelles and G. Boudjema, *Am. Nat.* **157**, 670 (2001).